Available online at www.sciencedirect.com

ScienceDirect

Mathematics and Computers in Simulation 106 (2014) 95–108

MATHEMATICS AND COMPUTERS IN SIMULATION

www.elsevier.com/locate/matcom

Original articles

A mathematical proof of how fast the diameters of a triangle mesh tend to zero after repeated trisection

Francisco Perdomo [a,b], Ángel Plaza [a,b,*], Eduardo Quevedo [c], José P. Suárez [a,d]

[a] *Division of Mathematics, Graphics and Computation (MAGiC). IUMA, Information and Communication Systems, University of Las Palmas de Gran Canaria (ULPGC), Spain*

[b] *Department of Mathematics, (ULPGC), Spain*

[c] *Department of Electronic and Automatic Engineering, ULPGC, Spain*

[d] *Department of Cartography and Graphic Engineering, ULPGC, Spain*

Received 6 May 2011; received in revised form 7 September 2013; accepted 10 August 2014

Available online 23 August 2014

Abstract

The Longest-Edge (LE) trisection of a triangle is obtained by joining the two points which divide the longest edge in three with the opposite vertex. If LE-trisection is iteratively applied to an initial triangle, then the maximum diameter of the resulting triangles is between two sharpened decreasing functions. This paper mathematically answers the question of how fast the diameters of a triangle mesh tend to zero as repeated trisection is performed, and completes the previous empirical studies presented in the MASCOT 2010 Meeting (Perdomo et al., 2010).

Keywords: Longest-edge; Triangle subdivision; Trisection; Mesh refinement; Finite element method

1. Introduction

Mesh refinement has been a constant area of research in applied mathematics and engineering applications [5,13,19,28]. For example, the longest-edge bisection guarantees the construction of high-quality triangulations [1,8,20,24–26]. The finite element method requires good-quality meshes (triangulations of surfaces) for the numerical algorithms to run. Although the requirements for meshes largely depend on the algorithm, the sharp angle conditions seem to be a common feature of particular importance in this context. See for example [23] for the introduction to the subject and [21] for the state of art.

More specifically, the objective is to construct a sequence of nested conforming meshes that are adapted to a given criterion. Nested sequences of triangles where each element in the sequence is a child of the parent triangle of the same sequence are of substantial interest in many areas, such as Finite Element Multigrid Methods, Image Multiresolutions,

* Correspondence to: Department of Mathematics, University of Las Palmas de Gran Canaria, 35017-Las Palmas de Gran Canaria, Spain. Tel.: +34 928458827; fax: +34 928458711.

E-mail address: aplaza@dmat.ulpgc.es (Á. Plaza).

http://dx.doi.org/10.1016/j.matcom.2014.08.002

0378-4754/

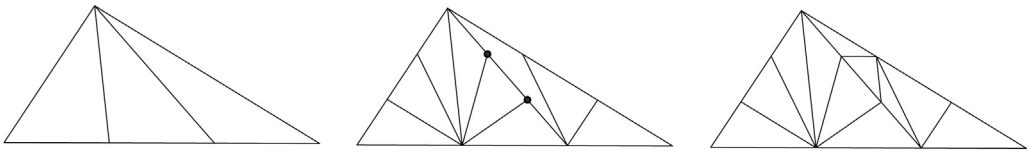

Fig. 1. Two steps in trisection by the longest edge. The conformity of the hanging nodes (in black) is assured by the local longest-edge trisection.

and others. In this sense, the generation of robust, reliable local mesh refinements for the production of meshes for finite element or finite difference methods is a significant area of study, together with the geometric and topological properties of the triangle or tetrahedral partitions [3,5,15,19,28].

Some of the properties of these longest-edge bisection based partitions and algorithms have already been indicated in the literature [14,18]. Two critical numerical indicators to guarantee quality meshes in FEM are minimum angle and the longest edge of triangles. For example, Rosenberg and Stenger [20] showed the non-degeneracy property for LE-bisection: if α_0 is the minimum angle of an initial given triangle, and α_n is the minimum interior angle in new triangles considered at iteration n, then $\alpha_n \geq \alpha_0/2$.

It is already well established that the assumption of regularity over the meshes [3], *i.e.*, the bounded ratio between the outer and inner diameters, leads to the convergence of standard finite element methods. As a consequence of the convergence of the diameters to zero, the bisection method has been proven to be useful in FEM for approximating solutions of differential equations [20,24,25].

Therefore, the problem of convergence of the triangulations generated by these methods is of interest and significance. The problem of convergence is one of how fast the diameters of the resulting triangles tend to zero as a repeated partition is performed. Kearfott in [6] proved the convergence of the diameters for the longest-edge bisection, showing that every two iterations of the longest-edge bisection method, the maximum lengths are reduced at least by a factor of $\sqrt{3}/2$. This yields to the bound $\delta_{2n} \leq \delta_0(\frac{\sqrt{3}}{2})^n$ where δ_n is the diameter of the mesh after n iterations of the longest-edge bisection. Afterwards, Stynes [24,25] and Adler [1] independently improved these bounds. They showed that $\delta_{2n} \leq \frac{\sqrt{3}}{2^n}\,\delta_0$ and $\delta_{2n+1} \leq \frac{1}{2^n}\,\delta_0$. It is interesting to note that these bounds cannot be improved as they hold for the case of the equilateral triangle.

Meanwhile, as all this previous background knowledge is well established in the case of the LE-bisection, proving it thus to be a highly robust and reliable method in practice, little evidence has been given with respect to the variant method of LE-trisection. An example of LE-trisection is shown in Fig. 1.

Partitions and local refinement algorithms are related [19]. For example, a local refinement has recently been proposed, based on LE-trisection [15]. Fig. 2 shows a typical refined mesh as obtained by this algorithm. Also the seven-triangle longest edge partition is related to the LE-trisection [9,16].

It has also been proved [11,14] that $\alpha_n \geq \alpha_0/c$, with $c = \frac{\pi/3}{\arctan(\sqrt{3}/11)}$, where, as was previously detailed, α_n is the minimum interior angle in the new triangles considered at iteration n, and α_0 the minimum angle of the initial given triangle.

Take a triangle with a longest edge length δ_0. The subdivision based on the trisection of the longest edge can be applied again to the newly generated triangles. Let δ_1 be the maximum length of the newly produced triangles. The repeated application of the partition generates an unstructured mesh of triangles. It can easily be seen that δ_n, when n extends to a level of refinement n, constitutes a decreasing sequence.

We have recently given numerical studies in [12] which corroborate the convergence of the longest-edge trisection. We studied 10 trisection iterations for 40 triangles with the aforementioned characteristics. The empirical results show the fidelity of the upper and lower bounds presented above, Fig. 3. In the figure, Kearfott-like bound $\delta_{2n} \leq \delta_0(\frac{\sqrt{7}}{3})^n$ is graphed. This bound may be obtained following a similar reasoning to [6] applied to the LE-trisection. The details for this bound are not given here. Notice that, Kearfott-like bound is not very accurate.

In this paper, we give accurate upper and lower bounds for the convergence speed in terms of diameter reduction. We then establish the rate of convergence for LE-trisection thereby filling the gap in the analysis of the diameter convergence for the LE-trisection of triangles. We answer the question: how fast do the diameters of a triangle mesh tend to zero after repeated trisection? We prove that the longest edge in the given meshes is bounded sharply on the upper limit. It is mathematically demonstrated that the upper bound is attained when an equilateral triangle is trisected.

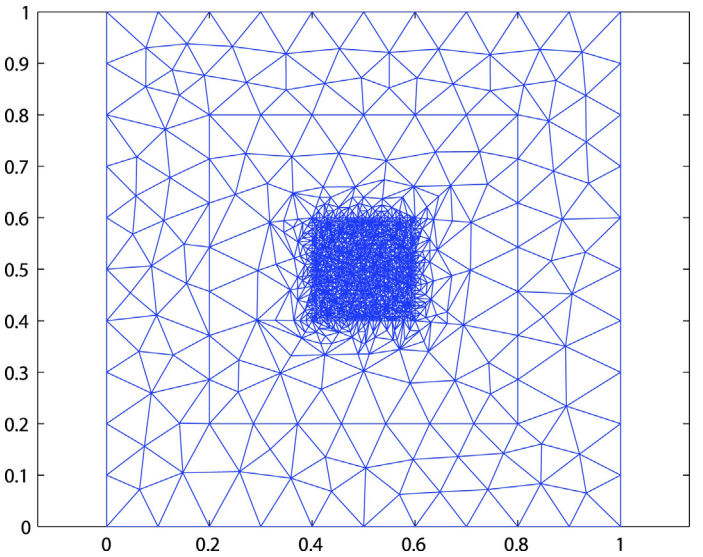

Fig. 2. Local refinement inside region (0.4, 0.4) – (0.6, 0.6). The final mesh has 2238 points and 4434 triangles.

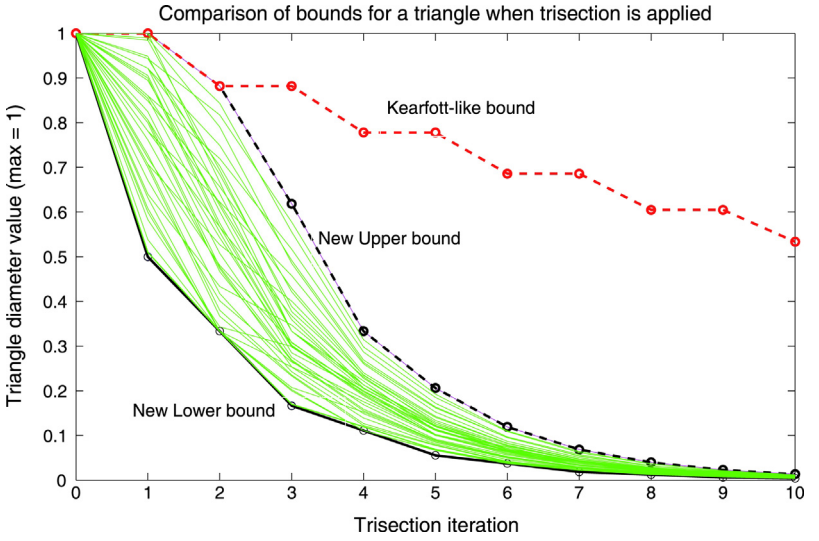

Fig. 3. Evolution of the ratio between the maximum LE after ten iterated trisections, and upper and lower bounds for 40 different initial triangles.

We also prove that for a general initial triangle with longest edge δ_0, if δ_n is the maximum diameter in nth iteration, then $\delta_{2n} \geq \frac{1}{3^n}\,\delta_0$ and $\delta_{2n+1} \geq \frac{1}{2.3^n}\,\delta_0$ for $n \geq 0$.

The structure of the paper is as follows. In Section 2, we introduce a scheme for normalizing triangles. This normalized region has also been used in the literature [2,17]. In Section 3, we present a hyperbolic geometry that will be used later. The main result of the paper is proved in Section 4. Section 5 is devoted to the proof of a lower bound of the diameters. Finally, a summarized version of some of the conclusions is given.

2. Introduction to triangle normalization

A method used in the literature of triangle mesh refinement is to normalize triangles [2,17]. The normalization process consists in applying several possible isometries and dilations to a triangle, matching its longest side with the segment whose endpoints are (0, 0) and (1, 0), and leaving its lower side to the left. Similar triangles are characterized by a unique complex number z in the normalized region, $\Sigma = \{0 < x \leq 1/2,\, y > 0,\, (x-1)^2 + y^2 \leq 1\}$.

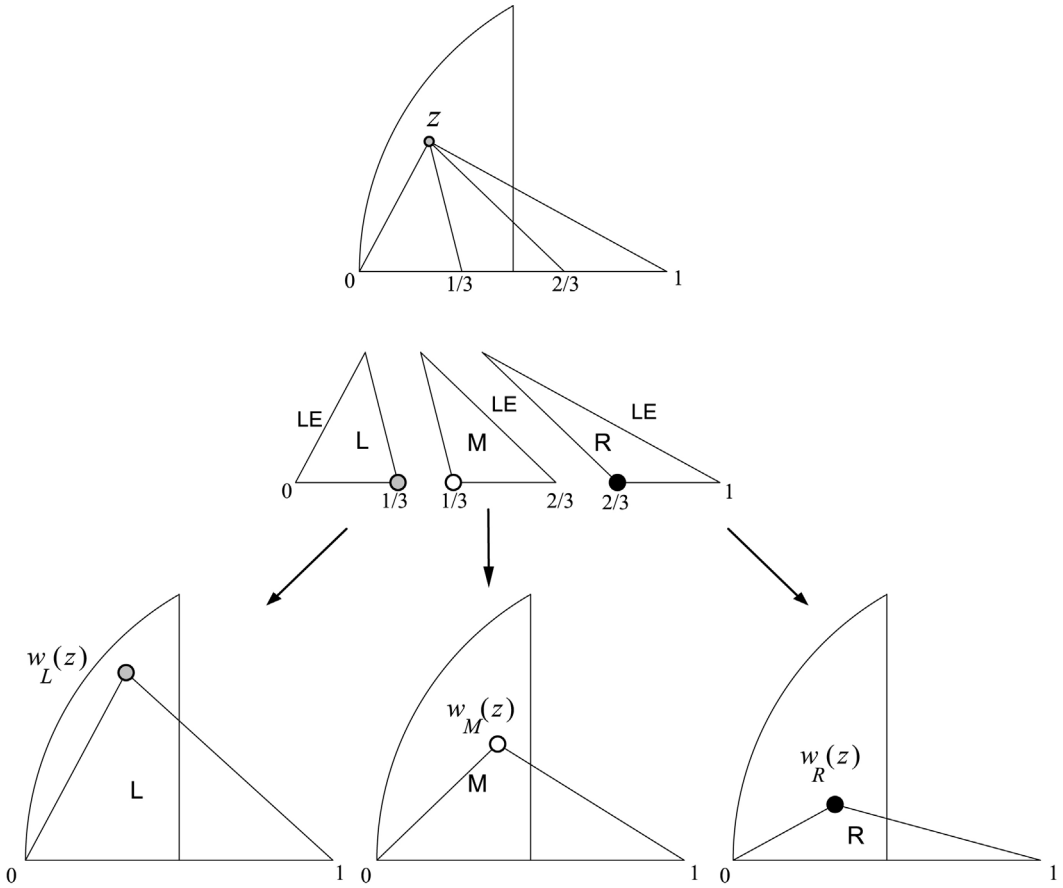

Fig. 4. Complex functions w_L, $w_M(z)$ and $w_R(z)$ in the trisection of a triangle given by point z.

Remember that the LE-trisection of a triangle is obtained by joining two equally spaced points on the longest edge of the triangle to the opposite vertex. Three new triangles are generated: the left (L), middle (M) and right (R) (on account of their positions) triangles. See Fig. 4.

The normalization of the left triangle L gives a complex number $w_L(z)$. In the same way the normalization of the middle triangle M gives a complex number $w_M(z)$ and the normalization of the right triangle R gives a complex number $w_R(z)$. Note that, the normalization process depends on which edge in each sub-triangle is the longest one. Fig. 4 shows how the normalization of the three subtriangles produced by the longest-edge trisection defines complex variable functions w_L, $w_M(z)$ and $w_R(z)$. In each sub-triangle, the longest edge is marked by LE and the opposite vertex is coloured. In this way, for an initial triangle with associated complex number z, we obtain three complex numbers $w_L(z)$, $w_M(z)$ and $w_R(z)$, corresponding to the final position of the opposite vertex to the longest edge of each sub-triangle, after they have been normalized.

The normalization process of the left, middle, and right triangles generated by the LE-trisection depends on the lengths of the sides of the initial triangle and their relative positions. Therefore, for each one of the functions $w_L(z)$, $w_M(z)$ and $w_R(z)$, there are zones in the normalized region where that function has a unique expression. The expressions of the piecewise functions $w_L(z)$, $w_M(z)$ and $w_R(z)$, are given in Figs. 5 and 6, where the boundaries between zones with different expressions are labelled.

By way of example, we reproduce the derivation of function $w_R(z)$ for z in the normalized region with $|z - \frac{2}{3}| \geq \frac{1}{3}$. See Fig. 7. The longest edge of the right triangle (triangle in grey in Fig. 7(a)) joins point (1, 0) to the affix of the complex number z and the shortest edge is the horizontal segment of length $\frac{1}{3}$. We translate through vector $(-1, 0)$ as in Fig. 7(b) and then the triangle is rotated so that the longest edge is over the real axis, see Fig. 7(c). Finally, the longest edge is normalized to 1 through a dilation of rate $\frac{1}{|z-1|}$ as depicted in Fig. 7(d).

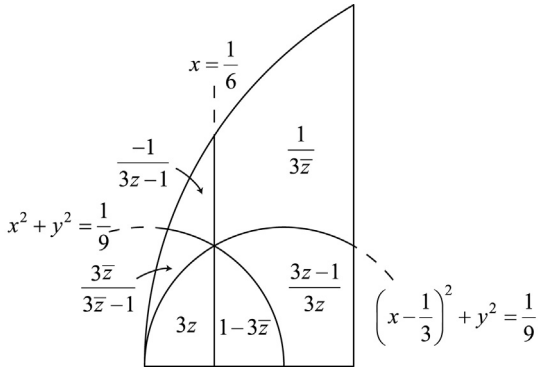

Fig. 5. Piecewise definition of complex function w_L.

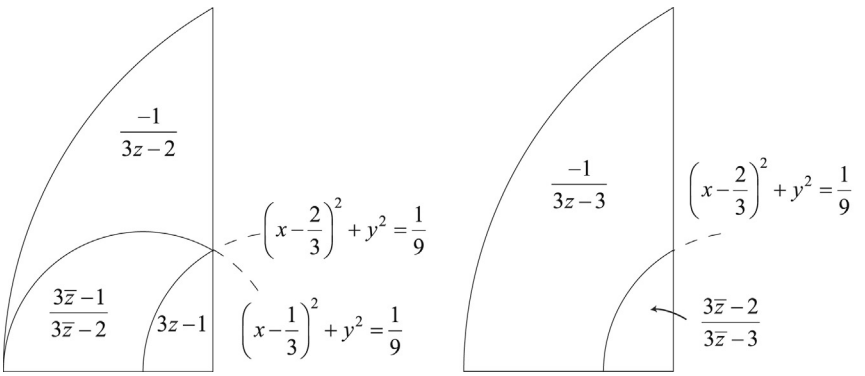

Fig. 6. Piecewise definition of complex functions w_M (left) and w_R (right).

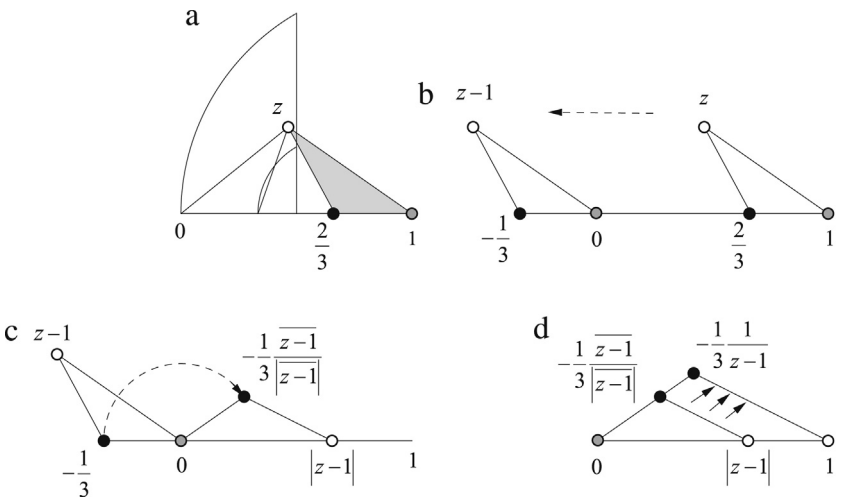

Fig. 7. Example of geometric transformations to obtain function $w_R(z)$.

3. Introduction to hyperbolic distance

We use the results of hyperbolic geometry and particularly the Poincare half-plane model [4,22,27] in this paper. The circumferences and straight lines appearing in w_L, w_M and w_R definitions are orthogonal to $y=0$, and are geodesics in the Poincare half-plane. The expressions that appear in w_L, w_M and w_R are isometries in the half-plane hyperbolic model since they have the form $m(z)=\frac{az+b}{cz+d}$ or $\bar{m}(z)=m(\bar{z})=\frac{a(-z)+b}{c(-z)+d}$ with real coefficients verifying $a\,d-b\,c>0$.

As it is known functions of the form $m(z)$ are called Möbius transformations, while those of the form $\bar{m}(z)$ are named anti-Möbius transformations [7].

The functions w_L, w_M and w_R are symmetrical to the circumferences (or the straight line) which appear on the boundary of two neighbouring zones of the normalized region. For example, the circumference $(x-\frac{2}{3})^2+y^2=\frac{1}{9}$ appears in the definition of w_R (Fig. 5). The inversion with respect to this circumference is expressed by $inv(z)=\frac{2-z-1}{3-z-2}$. Expressions of w_R are $w_R^{(1)}(z)=\frac{3-z-2}{3-z-3}$ and $w_R^{(2)}(z)=\frac{-1}{3z-3}$, and each one can be obtained by the composition of the inversion of with respect to the circumference with the other. That is $w_R^{(1)}(inv(z))=w_R^{(2)}(z)$, and $w_R^{(2)}(inv(z))=w_R^{(1)}(z)$.

Here, for convenience, we give some results for hyperbolic distance. If z_1 and z_2 are complex numbers with $\operatorname{Im} z_1>0$ and $\operatorname{Im} z_2>0$, then the hyperbolic distance d between z_1 and z_2 is defined by the formula

$$\cosh d(z_1,z_2)=1+\frac{|z_1-z_2|^2}{2\operatorname{Im} z_1\operatorname{Im} z_2} \tag{1}$$

and if z_1 and z_2 have the same real parts, then

$$d(z_1,z_2)=|\ln(\frac{\operatorname{Im} z_1}{\operatorname{Im} z_2})|. \tag{2}$$

The following property asserts that the three functions w_L, w_M and w_R do not increase the distance between points in the normalized region or space of triangles.

Lemma 1. *(Non-Increasing Property) Let W be any of the functions w_L, w_M and w_R . For any z_1 and z_2 in the normalized region,*

$$d(W(z_1),W(z_2))\le d(z_1,z_2), \tag{3}$$

where $d(\cdot,\cdot)$ denotes the hyperbolic distance on the half-plane.

Proof. If z_1 and z_2 are in a region with the same definition of W, then $d(z_1,z_2)=d(W(z_1),W(z_2))$, because W is an isometry on the half-plane hyperbolic model. Let us now suppose that z_1 and z_2 are not in a region with the same definition of W. We have two possibilities:

(1) z_1 and z_2 are in two regions with a common boundary. There exists z_1' in the region of z_2 with $W(z_1)=W(z_1')$ due to the symmetry of W with respect to the boundary. Let γ be the geodesic line that joins z_1 and z_2. γ intersects the boundary at a point, say z^*. Then $d(z_1,z_2)=d(z_1,z^*)+d(z^*,z_2)$ because the three points are in the same geodesic. $d(z_1,z^*)=d(z_1',z^*)$, since z_1 and z_1' are symmetrical points with respect to the boundary containing z^*. Therefore, by the triangular inequality,

$$d(z_1,z_2)=d(z_1,z^*)+d(z^*,z_2)=d(z_1',z^*)+d(z^*,z_2)>d(z_1',z_2).$$

Thus $d(W(z_1),W(z_2))=d(W(z_1'),W(z_2))=d(z_1',z_2)<d(z_1,z_2)$.

(2) z_1 and z_2 are in different regions without a common boundary. We may apply the previous process to bring both z_1 and z_2 into the same region. □

4. Proof of the upper bound

First, we study the case of the equilateral triangle. The theoretical interest of this case lies in giving the upper bound of the convergence rate for any other triangle. Let δ_n be the diameter of the triangle mesh after n iterated applications of the LE-trisection of an initial equilateral triangle with longest edge δ_0. We seek to obtain the values of δ_n.

To set up our result, we use an invariant defined for the classes of similar triangles, introduced by Stynes [25] and Adler [1]. For an arbitrary triangle Δ, $\Phi(\Delta)$ is the ratio between the area of Δ and the square of its longest edge, $\Phi(\Delta) = \text{area}(\Delta)/\delta^2$. Let z be the complex number associated to the triangle Δ. We obtain $\Phi(\Delta) = \frac{1}{2}\,\text{Im}\, z$. It follows that:

$$\delta = \sqrt{\frac{\text{area}(\Delta)}{\Phi(\Delta)}} = \sqrt{\frac{2 \cdot \text{area}(\Delta)}{\text{Im}\, z}}. \tag{4}$$

Note that, all the triangles in the nth iteration for the equilateral triangle have areas equal to $\frac{1}{3^n}\,\frac{\sqrt{3}}{4}\,\delta_0^2$. Then the maximum length will be given for the longest side of the triangle whose value z has the lowest imaginary part in that iteration.

The first values may be obtained computationally: we have $\delta_1 = \delta_0$, $\delta_2 = \frac{\sqrt{7}}{3}\delta_0$, $\delta_3 = \frac{\sqrt{31}}{9}\delta_0$ and finally $\delta_4 = \frac{1}{3}\delta_0$.

From the fifth iteration we obtain the complex number $\frac{29}{62} + \frac{3\sqrt{3}}{62}i$. And then, for $n \geq 5$:

$$\delta_n = \sqrt{\frac{2\,\frac{1}{3^n}\,\frac{\sqrt{3}}{4}\,\delta_0^2}{\frac{3\sqrt{3}}{62}}} = \frac{\sqrt{31}}{3^{(n+1)/2}}\,\delta_0. \tag{5}$$

Now, we prove our main theorem. Before, however, we need the concepts of *closed set for trisection* given by the following definition.

Definition 2. A region Ω is called a *closed region for trisection* if for all $z \in \Omega$, $w_L(z)$, $w_M(z)$ and $w_R(z)$ are in Ω too. These regions will also be called *closed regions*.

For a point z in the normalized region Σ, the set of points obtained by any composition of functions $w_L(z)$, $w_M(z)$ and $w_R(z)$ to any previous images, will be called *orbit* of z and it will represented by Γ_z. This definition may be expressed mathematically as follows.

Definition 3. For a point $z \in \Sigma$, we define $\Gamma_z^{(0)} = \{z\}$ and

$$\Gamma_z^{(n+1)} = w_L(\Gamma_z^{(n)}) \cup w_M(\Gamma_z^{(n)}) \cup w_R(\Gamma_z^{(n)}).$$

Then, the orbit of z is the set $\bigcup_{n\geq 0}\Gamma_z^{(n)}$.

For example if $\omega_1 = \frac{1}{3} + \frac{\sqrt{2}}{3}i$, then $\Gamma_{\omega_1} = \{\omega_1, \omega_2, \omega_3\}$, where $\omega_2 = \frac{1}{3} + \frac{\sqrt{2}}{6}i$, and $\omega_3 = \frac{4}{9} + \frac{\sqrt{2}}{9}i$. As a matter of fact, Γ_{ω_1} is a finite orbit and this fact will play an important role in the proofs presented in this paper. In fact, Γ_{ω_1} is the only finite orbit for the longest-edge trisection [10].

From the definition, it follows that the orbit of a point Γ_z is a closed region. However, outside the orbits there are other closed sets.

Proposition 4. *Let z be a complex number in the normalized region Σ. Let Ω be the intersection with Σ of the union of the hyperbolic circles with centres in Γ_z and with the same radius r. Then Ω is a closed set for the LE-trisection.*

Proof. Let ω be in Ω. By definition of orbit, there exists a z' in Γ_z such that $d(\omega, z') \leq r$. If W is any of the functions $w_L(z)$, $w_M(z)$ and $w_R(z)$, by the non-increasing property of Lemma 1, then $d(W(\omega), W(z')) \leq r$. Hence, $W(\omega) \in \Omega$ because $W(z') \in \Gamma_z$. □

For example, the union of the three circles C_1, C_2, and C_3 with respective hyperbolic centres ω_1, ω_2, and ω_3 and equal radius $r = \ln\sqrt{2}$ is a closed set for the previous Proposition. See Fig. 8.

Theorem 5. *Let Δ_0 be a triangle, not necessarily equilateral, with longest edge δ_0, and let Δ_n be any triangle generated in the n-th iteration of the LE-trisection. If δ_n denotes the longest edge of Δ_n, then $\delta_n \leq \frac{\sqrt{31}}{3^{(n+1)/2}}\delta_0$.*

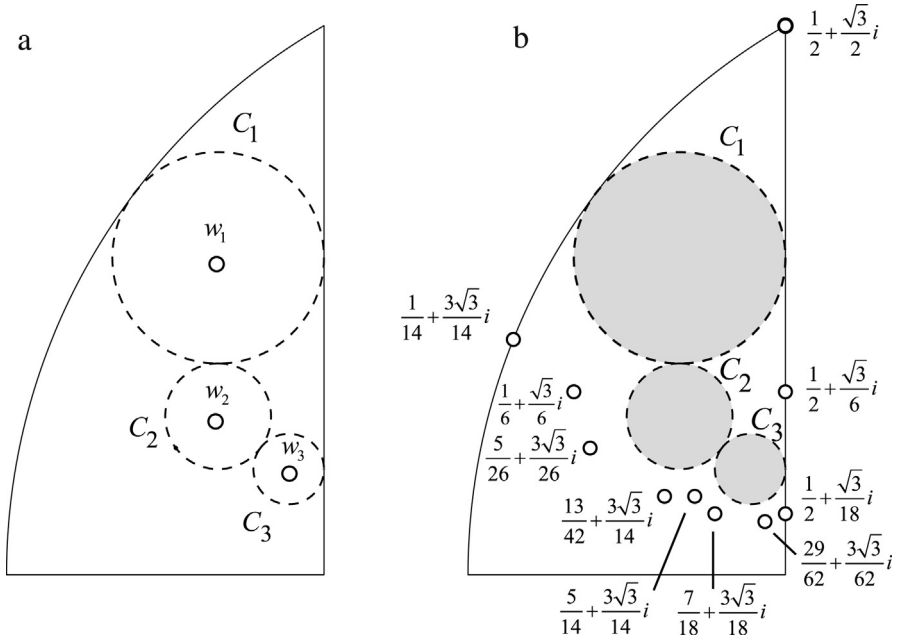

Fig. 8. (a) Circles C_1, C_2, and C_3 with respective hyperbolic centres ω_1, ω_2, and ω_3 (points in white) and with radius $\ln\sqrt{2}$. (b) Points in the orbit of $z_{eq} = \frac{1}{2} + \frac{\sqrt{3}}{2}i$ which are outside the circles C_1, C_2, and C_3.

Proof. Let z_0 be the associated complex number to Δ_0, and z_n the associated complex to Δ_n. Then,

$$\Phi(\Delta_0) = \frac{\text{area}(\Delta_0)}{\delta_0^2} = \frac{\operatorname{Im} z_0}{2},$$

$$\Phi(\Delta_n) = \frac{\text{area}(\Delta_n)}{\delta_n^2} = \frac{\operatorname{Im} z_n}{2},$$

and $\text{area}(\Delta_n) = \frac{1}{3^n}\,\text{area}(\Delta_0)$. Therefore, the statement of the theorem is equivalent to $\frac{\operatorname{Im} z_0}{\operatorname{Im} z_n} \leq \frac{31}{3}$.

We proceed by covering the normalized region with closed sub-regions, where the quotient $\frac{\operatorname{Im} z_0}{\operatorname{Im} z_n}$ is bounded by a value less than or equal to the desired one.

First we consider the closed region given by the union of the three hyperbolic circles C_1, C_2 and C_3 with equal radius $r = \ln\sqrt{2}$ as in Fig. 8. If z_0 is a complex number inside one of these circles, C_1, C_2 or C_3, then $\frac{\operatorname{Im} z_0}{\operatorname{Im} z_n} \leq 6$ because every complex z in the union of these circles verifies that $\frac{1}{9} \leq \operatorname{Im} z \leq \frac{2}{3}$.

Effectively, the top point z_T of circle C_1 with centre ω_1 verifies

$$\ln\sqrt{2} = \ln\left(\frac{\operatorname{Im} z_T}{\operatorname{Im}\omega_1}\right) = \ln\left(\frac{\operatorname{Im} z_T}{\sqrt{2}/3}\right),$$

since $\operatorname{Re} z_T = \operatorname{Re}\omega_1 = \frac{1}{3}$ and $d(z_1, z_2) = |\ln(\frac{\operatorname{Im} z_1}{\operatorname{Im} z_2})|$, for z_1 and z_2 with the same real parts. Therefore $\operatorname{Im} z_T = \frac{2}{3}$. Similarly, for the bottom point z_B of C_3 with centre ω_3, it holds that

$$\ln\sqrt{2} = \ln\left(\frac{\operatorname{Im}\omega_3}{\operatorname{Im} z_B}\right) = \ln\left(\frac{\sqrt{2}/9}{\operatorname{Im} z_B}\right),$$

and then $\operatorname{Im} z_B = \frac{1}{9}$.

Let Γ_{eq} be the sub-set of points of the orbit of $\frac{1}{2} + \frac{\sqrt{3}}{2}i$ outside the circles C_1, C_2 and C_3 (white dots in Fig. 9). Let us consider the union of C_1, C_2, C_3 and the hyperbolic circles of radius $\ln\sqrt{3}$ with centres in Γ_{eq} and let Ω_1 be the intersection of this union with the normalized region. See Fig. 9. Region Ω_1 is closed for trisection by Proposition 4. If z_0 is in Ω_1, then $\frac{\operatorname{Im} z_0}{\operatorname{Im} z_n} \leq \frac{31}{3}$. Effectively, we consider two cases:

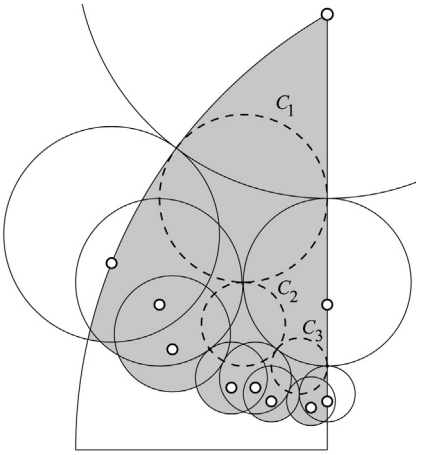

Fig. 9. Region Ω_1 in grey, hyperbolic circumferences C_1, C_2 and C_3 in dotted lines, and hyperbolic circumferences with radius $\ln\sqrt{3}$ and centres in Γ_{eq}, white dots.

CASE I: let z_0 be in Ω_1 with $0 < \operatorname{Im} z_0 \leq \frac{27}{62}$, in grey in Fig. 10. The lowest imaginary part in Σ is given by the bottom point, z_B, of the hyperbolic circumference with centre $\frac{29}{62} + \frac{3\sqrt{3}}{62}i$ and radius $\ln\sqrt{3}$. Recall that for z_1 and z_2 with the same real parts, $d(z_1, z_2) = |\ln(\frac{\operatorname{Im} z_1}{\operatorname{Im} z_2})|$. Then, the hyperbolic distance from z_B to the centre is $\ln(\frac{3\sqrt{3}/62}{\operatorname{Im} z_B}) = \ln\sqrt{3}$, and therefore $\operatorname{Im} z_B = \frac{3}{62}$. It follows that the bound $\frac{\operatorname{Im} z_0}{\operatorname{Im} z_n} \leq \frac{27/62}{3/62} = 9 < \frac{31}{3}$. □

CASE II: now let $\Omega_2 \subset \Omega_1$ be comprised of the circles C_1, C_2 and C_3 and the regions, tangent cones between two tangent geodesics to these circles from points in Γ_{eq}. See Fig. 11. If Ω_2 is a closed region then $\frac{\operatorname{Im} z_0}{\operatorname{Im} z_n} \leq \frac{31}{3}$, because the maximum and the minimum imaginary parts are $\frac{\sqrt{3}}{2}$ and $\frac{3\sqrt{3}}{62}$, respectively. It only remains to prove that Ω_2 is a closed region.

The union of C_1, C_2 and C_3 is a closed region. We only have to see that the image of every tangent cone by w_L, w_M or w_R is included in Ω_2. We can distinguish three cases:

(1) the restriction to a tangent cone of w_L, w_M or w_R is a unique Möbius or anti-Möbius function and the image of the base point of the tangent cone is in Γ_{eq}. In this case, the image of the tangent cone is also a tangent cone. This is

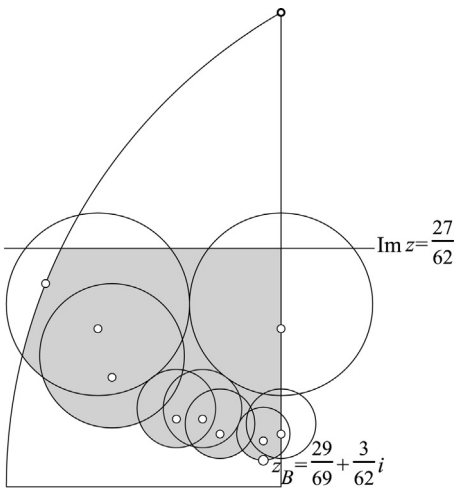

Fig. 10. Region of Ω_1 with $\operatorname{Im} z \leq \frac{27}{62}$. The bottom point z_B is labelled.

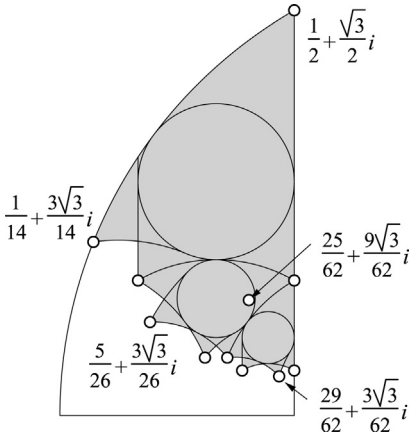

Fig. 11. Region Ω_2 (in grey) comprised of circles C_1, C_2 and C_3 and the zones between two tangent geodesics to these circles from points in Γ_{eq}.

because Möbius maps transform circumferences within circumferences, and preserve the angles, incidences and tangencies;

(2) the only function for which the restriction to a tangent cone has two different expressions is w_L. That is, the tangent cone overlaps the boundary of two zones with different expressions for w_L. This only happens for the two tangent cones with respective base points $\frac{5}{26}+\frac{3\sqrt{3}}{26}i$ and $\frac{1}{14}+\frac{3\sqrt{3}}{14}i$. See Fig. 12 where these points are in black, and also the boundary lines of the piecewise definition of function w_L are bold lines.

First, we study the cone with base point $\frac{5}{26}+\frac{3\sqrt{3}}{26}i$. By the symmetry of w_L with respect to the boundary curve $x^2+y^2=\frac{1}{9}$, the image of this tangent cone is included within the images of two other tangent cones and the circle C_2, which are in Ω for the previous proposal. The image of the point $\frac{5}{26}+\frac{3\sqrt{3}}{26}i$ by w_L is highlighted in black in Fig. 13.

Second, we consider the tangent cone with base point $\frac{1}{14}+\frac{3\sqrt{3}}{14}i$. We use that the region in which $w_L(z)=\frac{1}{3-z}$ is a closed region for w_L. See Fig. 14(b). By the symmetry of w_L with respect to the boundary line $x=\frac{1}{6}$, the image of this tangent cone is included within the image of this invariant region which is in Ω_2. See Fig. 14(a).

(3) It may also occur that the image of the base point is in C_1, C_2 or C_3. This occurs for function w_M and the tangent cones with base points $\frac{1}{14}+\frac{3\sqrt{3}}{14}i$, $\frac{5}{26}+\frac{3\sqrt{3}}{26}i$ or $\frac{29}{62}+\frac{3\sqrt{3}}{62}i$. The images of these three points are $\frac{25}{62}+\frac{9\sqrt{3}}{62}i$ which

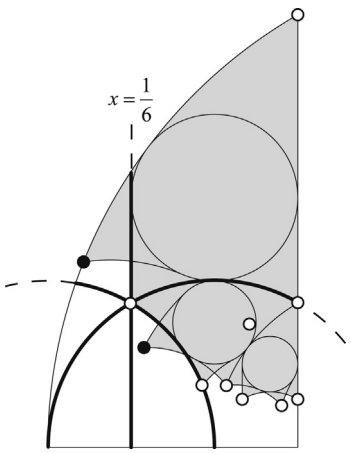

Fig. 12. Points with tangent cones where function w_L has two different expressions, in black. Bold lines are the boundary lines in the piecewise definition of w_L.

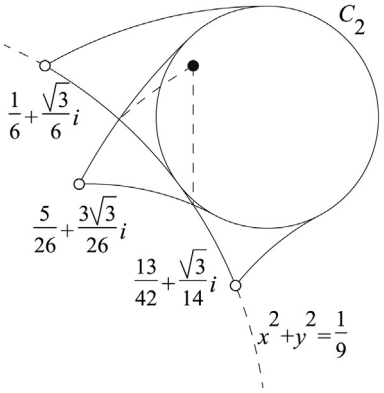

Fig. 13. The image by w_L of the tangent cone with base point $\frac{5}{26}+\frac{3\sqrt{3}}{26}i$ is included within the images of two other tangent cones and the circle C_2. The image of the point $\frac{5}{26}+\frac{3\sqrt{3}}{26}i$ by w_L is highlighted in black.

is inside C_2. Since the restriction of w_M to these tangent cones is a conformal map, then the images are tangent cones to C_1 with base point $\frac{25}{62}+\frac{9\sqrt{3}}{62}i$. In any case the images are in Ω_2. See Fig. 15.

Finally, we have to study the lowest part of the normalized region not included in Ω_1. The points of Γ_{eq} are in the hyperbolic circumferences of radius $\ln(\frac{\sqrt{2}+\sqrt{6}}{2})$ with centres in $\frac{1}{3}+\frac{\sqrt{2}}{3}i$, $\frac{1}{3}+\frac{\sqrt{2}}{6}i$ and $\frac{4}{9}+\frac{\sqrt{2}}{9}i$. Let Ω_3 now be the zone in the normalized region below these circumferences. See Fig. 16.

We will show that if $z_0 \in \Omega_3$, then $\frac{\operatorname{Im} z_0}{\operatorname{Im} z_n} < 5 < \frac{31}{3}$. Effectively, the straight line $y=mx$ through the origin cuts the circumference $(x-1)^2+y^2=1$ at point $\frac{2}{m^2+1}+\frac{2m}{m^2+1}i$. For $m \geq \sqrt{3}$, this point is on the arc of the normalized region, and for $m \geq 3\sqrt{3}$ this point is in Ω_3. The hyperbolic distance d of this intersection to the centre of the hyperbolic circumference C_1, $w_1=\frac{1}{3}+\frac{\sqrt{2}}{3}i$, verifies $\cosh d = \frac{m^2+9}{4\sqrt{2}m} \geq 1$. The union of the three hyperbolic circles with centres $w_1=\frac{1}{3}+\frac{\sqrt{2}}{3}i$, $w_2=\frac{1}{3}+\frac{\sqrt{2}}{6}i$ and $w_3=\frac{4}{9}+\frac{\sqrt{2}}{9}i$, of radius d is a closed region. Let z_0 be the top point in the boundary of this union of circles (see Fig. 16) inside the normalized region. In the worst case, $\operatorname{Im} z_0 = \frac{2m}{m^2+1}$ and $\operatorname{Im} z_n$ is equal to

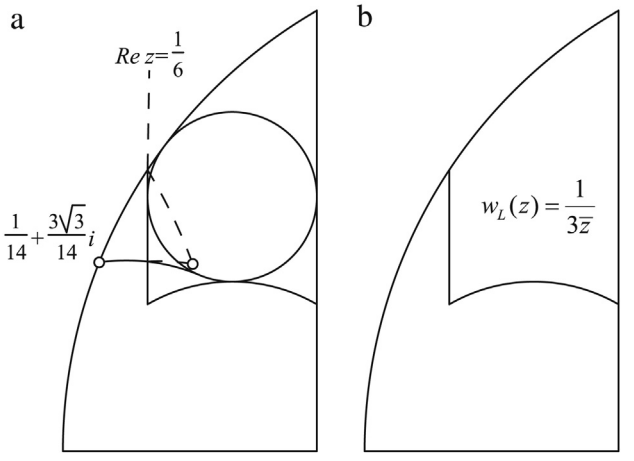

Fig. 14. (a) The image by w_L of the tangent cone with base point $\frac{1}{14}+\frac{3\sqrt{3}}{14}i$ is included in Ω_2, (b) sub-region where $w_L(z)=\frac{1}{3-z}$.

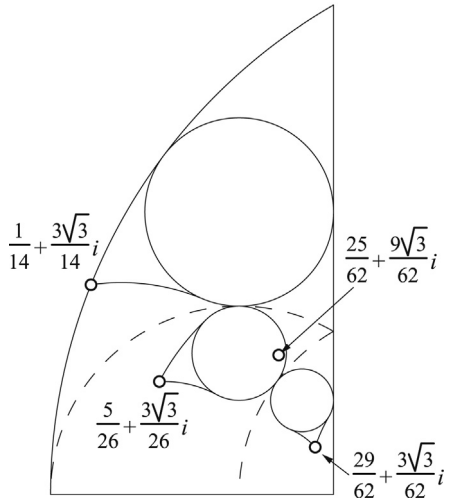

Fig. 15. The tangent cones with base points $\frac{1}{14}+\frac{3\sqrt{3}}{14}i$, $\frac{5}{26}+\frac{3\sqrt{3}}{26}i$ and $\frac{29}{62}+\frac{3\sqrt{3}}{62}i$ translate through function w_M to the tangent cone to C_1 with base point $\frac{25}{62}+\frac{9\sqrt{3}}{62}i$.

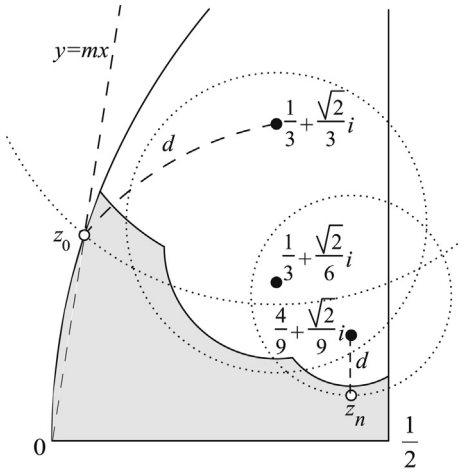

Fig. 16. Region Ω_3 (in grey) is the zone in normalized region below the hyperbolic circumferences with centres in $\omega_1=\frac{1}{3}+\frac{\sqrt{2}}{3}i$, $\omega_2=\frac{1}{3}+\frac{\sqrt{2}}{6}i$ and $\omega_3=\frac{4}{9}+\frac{\sqrt{2}}{9}i$ and radius $\ln(\frac{\sqrt{2}+\sqrt{6}}{2})$.

the lowest ordinates of the circumference with its centre at $w_3=\frac{4}{9}+\frac{\sqrt{2}}{9}i$ and radius d. Since z_n and w_3 have the same real parts, then $d=d(z_n,w_3)=\ln(\frac{\sqrt{2}/9}{\operatorname{Im} z_n})$ and then $\operatorname{Im} z_n=\frac{\sqrt{2}}{9}e^{-d}$. Therefore, since $m\geq 3\sqrt{3}$, we conclude that

$$\frac{\operatorname{Im} z_0}{\operatorname{Im} z_n}\leq\frac{9}{4}\,\frac{m^2+9+\sqrt{m^4-14m^2+81}}{m^2+1}\leq\frac{27(\sqrt{3}+3)}{28}<5<\frac{31}{3}.$$

This completes the proof. □

5. Proof of the lower bound

Proposition 6. *Let Δ_0 be a triangle with longest edge δ_0 . Let Δ_n be any triangle generated in the iteration n with longest edge δ_n . Then $\delta_{2n}\geq\frac{1}{3^n}\,\delta_0$ and $\delta_{2n+1}\geq\frac{1}{2\cdot 3^n}\,\delta_0$ for $n\geq 0$.*

Proof. Let z_0 be the associated complex number to triangle Δ_0, and let z_n be the associated complex number to Δ_n. Remember that $\delta_n = \sqrt{\frac{2\cdot\text{area}(\Delta_n)}{\text{Im}\, z_n}}$. To prove that $\delta_{2n} \geq \frac{1}{3^n}\,\delta_0$ and $\delta_{2n+1} \geq \frac{1}{2\cdot 3^n}\,\delta_0$ is equivalent to proving that there are z_{2n} and z_{2n+1} with $\frac{\text{Im}\, z_0}{\text{Im}\, z_{2n}} \geq 1$ and $\frac{\text{Im}\, z_0}{\text{Im}\, z_{2n+1}} \geq \frac{3}{4}$ for any $n \geq 0$. However, it is true that $\frac{\text{Im}\, z}{\text{Im}\, w_R(z)} \geq \frac{3}{4}$ for every z in the normalized region. Moreover, $\frac{\text{Im}\, z}{\text{Im}\, w_R^2(z)} \geq 1$ for every z in the normalized region too. Indeed, if $w = \frac{az+b}{cz+d}$ or $w = \frac{a(--z)+b}{c(--z)+d}$ with $ad - bc > 0$, then

$$\frac{\text{Im}\, z}{\text{Im}\, w} = \frac{c^2}{|ad-bc|}\,[(x - \frac{d}{c})^2 + y^2].$$

A few computations allow us to check these bounds for w_R and w_R^2. To this purpose, we should consider that for z in the normalized region is $w_R(z) = \frac{3\bar{z}-2}{3\bar{z}-3}$ if $|z - \frac{2}{3}| \leq \frac{1}{3}$; and $w_R(z) = \frac{-1}{3z-3}$ if $|z - \frac{2}{3}| \geq \frac{1}{3}$. Let the assertion be true for $n-1$. Then there are z_{2n-2} and z_{2n-1} with $\frac{\text{Im}\, z_0}{\text{Im}\, z_{2n-2}} \geq 1$ and $\frac{\text{Im}\, z_0}{\text{Im}\, z_{2n-1}} \geq \frac{3}{4}$. Therefore, we get $z_{2n} = w_R^2(z_{2n-2})$ and $z_{2n+1} = w_R^2(z_{2n-1})$ with $\frac{\text{Im}\, z_0}{\text{Im}\, z_{2n}} = \frac{\text{Im}\, z_0}{\text{Im}\, z_{2n-2}} \cdot \frac{\text{Im}\, z_{2n-2}}{\text{Im}\, z_{2n}} \geq 1$ and $\frac{\text{Im}\, z_0}{\text{Im}\, z_{2n+1}} = \frac{\text{Im}\, z_0}{\text{Im}\, z_{2n-1}} \cdot \frac{\text{Im}\, z_{2n-1}}{\text{Im}\, z_{2n+1}} \geq \frac{3}{4}$. The proposition is proved by induction. □

6. Conclusions

In this paper, we have used hyperbolic geometry to prove sharpened bounds for the diameters of the triangles generated by the longest-edge trisection. We then delimit the rate of convergence for this refinement method. This paper is a detailed and rigorous response to the question of how fast the diameters of a triangle mesh tend to zero after repeated trisection is performed, as previously carried out for the longest-edge bisection by Stynes, Adler and Kearfott. The mathematical proofs given here complete previous empirical studies and show that the longest-edge trisection is a robust method for the problem of triangle mesh refinement.

Acknowledgement

This work has been supported in part by the CICYT Project number MTM2008-05866-C03-02/MTM from the Spanish Ministerio de Educación y Ciencia.

References

[1] A. Adler, On the bisection method for triangles, Math. Comp. 40 (162) (1983) 571–574.
[2] C. Gutiérrez, F. Gutiérrez, M.-C. Rivara, Complexity of bisection method, Theoret. Comput. Sci. 382 (2) (2007) 131–138.
[3] A. Hannukainen, S. Korotov, M. Křížek, On global and local mesh refinements by a generalized conforming bisection algorithm, J. Comput. Appl. Math. 235 (2) (2010) 419–436.
[4] B. Iversen, Hyperbolic Geometry, Cambridge University Press, 1992.
[5] M. Jones, P. Plassmann, Adaptive refinement of unstructured finite-element meshes, Finite Elem. Anal. Des. 25 (1–2) (1997) 41–60.
[6] B. Kearfott, A proof of convergence and error bound for the method of bisection in $\mathbb{R}^n$, Math. Comp. 32 (144) (1978) 1147–1153.
[7] V.G. Kim, Y. Lipman, X. Chen, T. Funkhouser, Möbius Transformations For Global Intrinsic Symmetry Analysis, Eurographics Symposium on Geometry Processing 2010, vol. 29, 2010, Olga Sorkine and Bruno Lévy (Guest Editors), Number 5.
[8] S. Korotov, M. Křížek, A. Kropác, Strong regularity of a family of face-to-face partitions generated by the longest-edge bisection algorithm, Comput. Math. Math. Phys. 49 (9) (2008) 1687–1698.
[9] A. Márquez, A. Moreno-González, A. Plaza, J.P. Suárez, The seven-triangle longest-side partition of triangles and mesh quality improvement, Finte Elem. Anal. Des. 44 (12–13) (2008) 748–758.
[10] F. Perdomo, Dynamics of the longest-edge partitions in a triangle space endowed with an hyperbolic metric (Ph.D. thesis), (in Spanish) Las Palmas de Gran Canaria, 2013.
[11] F. Perdomo, A. Plaza, Proving the non-degeneracy of the longest-edge trisection by a space of triangular shapes with hyperbolic metric, Appl. Math. Comput. 221 (15) (2013) 424–432.
[12] F. Perdomo, E. Quevedo, A. Plaza, J.P. Suárez, Results on the Convergence of the Longest-edge Trisection Method for Triangles, Proceeding of MASCOT10-IMACS/ISGG Workshop (2010).
[13] A. Plaza, G.F. Carey, Local refinement of simplicial grids based on the skeleton, Appl. Numer. Math. 32 (2) (2000) 195–218.
[14] A. Plaza, S. Falcón, J.P. Suárez, On the non-degeneracy property of the longest-edge trisection of triangles, Appl. Math. Comput. 216 (3) (2010) 862–869.

[15] A. Plaza, S. Falcón, J.P. Suárez, P. Abad, A local refinement algorithm for the longest-edge trisection of triangle meshes, Math. Comput. Simulation 82 (12) (2012) 2971–2981.
[16] A. Plaza, A. Márquez, A. Moreno-González, J.P. Suárez, Local refinement based on the 7-triangle longest-edge partition, Math. Comput. Simulation 79 (8) (2009) 2444–2457.
[17] A. Plaza, J.P. Suárez, G.F. Carey, A geometric diagram and hybrid scheme for triangle subdivision, Comput. Aided Geom. Design 24 (1) (2007) 19–27.
[18] A. Plaza, J.P. Suárez, M.A. Padrón, S. Falcón, D. Amieiro, Mesh quality improvement and other properties in the four-triangles longest-edge partition, Comput. Aided Geom. Design 21 (4) (2004) 353–369.
[19] M.-C. Rivara, Mesh refinement processes based on the generalized bisection of simplices, SIAM J. Numer. Anal. 21 (3) (1984) 604–613.
[20] I.G. Rosenberg, F. Stenger, A lower bound on the angles of triangles constructed by bisecting the longest side, Math. Comp. 29 (130) (1975) 390–395.
[21] J.R. Shewchuk, What Is a Good Linear Finite Element? Interpolation, Conditioning, Anisotropy, and Quality Measures, unpublished preprint, 2002; available at http://www.cs.cmu.edu/ jrs/jrspapers.html
[22] S. Stahl, The Poincaré Half-Plane, Jones & Bartlett Learning, 1993.
[23] G. Strang, G.J. Fix, An Analysis of the Finite Element Method, Prentice-Hall, Englewood Cliffs, N.J, 1973.
[24] M. Stynes, On faster convergence of the bisection method for certain triangles, Math. Comp. 33 (146) (1979) 717–721.
[25] M. Stynes, On faster convergence of the bisection method for all triangles, Math. Comp. 35 (152) (1980) 1195–1201.
[26] J.P. Suárez, T. Moreno, P. Abad, A. Plaza, Properties of the longest-edge n-section refinement scheme for triangular meshes, Appl. Math. Lett. 25 (12) (2012) 2037–2039.
[27] G. Toth, Glimpses of Algebra an Geometry, Springer, 2002.
[28] O. Zienkiewicz, J. Zhu, Adaptivity and mesh generation, Internat. J. Numer. Methods Engrg. 32 (4) (1991) 783–810.